

# RSC Advances



This is an *Accepted Manuscript*, which has been through the Royal Society of Chemistry peer review process and has been accepted for publication.

*Accepted Manuscripts* are published online shortly after acceptance, before technical editing, formatting and proof reading. Using this free service, authors can make their results available to the community, in citable form, before we publish the edited article. This *Accepted Manuscript* will be replaced by the edited, formatted and paginated article as soon as this is available.

You can find more information about *Accepted Manuscripts* in the [Information for Authors](#).

Please note that technical editing may introduce minor changes to the text and/or graphics, which may alter content. The journal's standard [Terms & Conditions](#) and the [Ethical guidelines](#) still apply. In no event shall the Royal Society of Chemistry be held responsible for any errors or omissions in this *Accepted Manuscript* or any consequences arising from the use of any information it contains.



Journal Name

ARTICLE

## Biocomposites for wound-healing based on sol-gel magnetite

Volodina K.V.<sup>a,b</sup>, Drozdov A.S.<sup>a</sup>, Vinogradov Vasily V.<sup>a</sup>, and Vinogradov Vladimir V.<sup>a\*</sup>Received 00th January 20xx,  
Accepted 00th January 20xx

DOI: 10.1039/x0xx00000x

[www.rsc.org/](http://www.rsc.org/)

Currently, efficient wound-healing materials are booming due to increasing health care costs, world population aging, but also because of a sharp increase in the incidence of diabetes and obesity. Exacting demands are placed upon modern wound-healing materials as these should affect all stages of healing by accelerating them. In this paper, we demonstrate for the first time that the drug entrapped magnetite xerogels can be effectively used for this purpose. To prepare a healing biocomposite, we have combined four materials in a magnetite matrix: chlorhexidine digluconate as an antimicrobial agent, lidocaine as a painkiller, prednisolone as an anti-inflammatory agent and chymotrypsin as a necrolytic agent. Compared to the control group, the wound healing rate with a biocomposite exhibited a ~1.5-fold increase (21 and 14 days for complete healing, respectively). Moreover application of magnetite – based biocomposite provided strong scar size decrease. Characteristics of magnetite matrix as well as those of the healing xerogels derived from it are fully described by XRD, XPS, SEM, TEM and N<sub>2</sub> physisorption analysis.

### Introduction

To date, more than \$25 billion in the USA alone is spent on the treatment of chronic wounds, and this amount is growing fast due to increasing health care costs, population aging, but also because of a sharp increase in the incidence of diabetes and obesity. The global market of wound-healing materials in 2010 alone amounted to \$15.3 billion [1]. The reason for this is obvious: it is known that every year one tenth of the world's population suffers some kind of injury, and the number of victims increases sharply during hostilities, acts of terrorism and natural disasters. Along with wound healing another huge problem is skin scarring, a \$12 billion annual market. Due to exceptional economic and social importance of wound healing and scar treatment, new knowledge in this field attracts a high level of attention and resources to understand biological mechanisms underlying cutaneous wound complications. From this point of view, the new materials, which not only possess a high healing rate, but also significantly reduce skin scarring, could be an ideal system for wound healing.

Traditional dressing materials include woven textiles of natural and synthetic origin [2]. Clinicians require more functional biomaterials which is able to not only supports structural, physical and mechanical properties, but also controls biological and therapeutic processes during healing.

Nanomaterials have attracted great attention of doctors and clinicians in recent years because of the wide range of their

possible use in biomedicine [3]. The potential success of nanomaterials in tissue engineering provided strong foundation for future applications in wound management. Clinical approaches to wound repair and burn management are experiencing a new stage based on the use of more efficient composite nanomaterials [4].

Among nanomaterials, metal nanoparticles [5] and oxides [6] are of significant importance in wound healing. In particular, nanocrystalline silver is one of the most important components in wound dressing materials due to a broad spectrum of antibacterial activity [7]. Copper nanoparticles exhibit a pronounced biological activity, including bacteriostatic and bactericidal effects [8]. Iron nanoparticles in the form of an aqueous suspension for subcutaneous administration, and in the form of ointment, when applied to a wound, have a wound-healing effect [9]. Among the oxides, alumina and ferric are of the greatest practical application, because these are the only metal oxides approved by FDA for parenteral injection into the human body. Alumina (mainly boehmite) has numerous applications as the most common vaccine adjuvant [10], while ferric (mainly maghemite or magnetite) is the component for magnetic resonance imaging and anemia drug FeraHeme® [11]. Both are biocompatible and biodegradable [12,13]. While wound-healing properties of sol-gel alumina and biocomposites thereof were already studied in our previous work [14], wound-healing properties of ferric have not yet been investigated in detail. In Ref. [9], efficiency of the thrombin conjugated  $\gamma$ -Fe<sub>2</sub>O<sub>3</sub> nanoparticles for incisional wound healing was shown. But application of magnetite (Fe<sub>3</sub>O<sub>4</sub>) is more reasonable since, as it was shown [15], magnetite causes smaller toxicity effects in cultured A549 cells (the human lung epithelial cell line) in comparison to maghemite (Fe<sub>2</sub>O<sub>3</sub>).

<sup>a</sup> *a Laboratory of Solution Chemistry of Advanced Materials and Technologies, ITMO University, St. Petersburg, 197101, Russian Federation  
vinogradoffs@mail.ru;*

<sup>b</sup> *b Ivanovo State University of Chemistry and Technology, Ivanovo, 153000, Russian Federation;  
See DOI: 10.1039/x0xx00000x*

The biggest advantages of wound-healing composites could be to the versatility of biodegradable nanoparticles and controlled release to wound site, mimicking small nanofactory as delivery vehicle [16] therapy. Following modern requirements to the wound healing materials, they should provide bactericidal, anesthetic, anti-inflammatory and necrolytic properties [17]. Advanced functionality of biocomposites should be provided by controlled drug release as optimally needed for wound healing process [18]. In an ideal situation, the maximum dose of painkiller should release during the first minutes after the damage has been caused. The release of an antibacterial agent should proceed with a high initial portion with following aligning to prevent the formation of colonies of bacteria, both directly at the wound and in the dressing material. Release of necrolytic and anti-inflammatory agents should proceed slowly to provide a long-term effect.

In the present work we demonstrate new biocomposites based on sol-gel magnetite, which potentially can meet modern requirements for wound healing providing both high rate of healing and decrease of scar size due to controlled drug release as needed. For this aim, a group of drugs including lidocaine (LD), as a painkiller known for some beneficial effects on wound healing [19], chlorhexidine digluconate (CH), for wounds infection control, chymotrypsin (CHRT), as a necrolytic agent to prevent the formation of a scab and tissue necrosis while making healing process faster, [20] and prednisolone (PRD), as anti-inflammatory agent, entrapped in a magnetite sol-gel dressing film has been applied. The biocomposite exhibited exceptional wound healing properties after operation. For comparison, we have studied the wound-healing properties for both magnetite matrix and individual drugs in solution. To the best of our knowledge, this is the first example of wound-healing effects shown for iron oxide materials. It is important to note here that magnetite nanoparticles effect on morphology and adhesion properties of fibroblast cells and widely used in in vitro experiments relevant to magnetic tissue engineering [21,22].

## Materials and Methods

### Chemicals

Iron (II) chloride tetrahydrate, iron (III) chloride hexahydrate, aqueous solution of ammonia (25%), lidocaine hydrochloride 2% solution, chymotrypsin (cat. No. C4129), 20% solution of chlorhexidine digluconate and prednisolone were all obtained from Sigma-Aldrich. Glycine buffer (pH = 7.4) was prepared from glycine solutions (0.05 M; from Sigma-Aldrich) with desired volumes of 1.0 M NaOH.

### Synthesis of magnetite hydrosol

2.5 g  $\text{FeCl}_2 \cdot 4\text{H}_2\text{O}$  and 5 g  $\text{FeCl}_3 \cdot 6\text{H}_2\text{O}$  was dissolved in 100 mL of deionized water under constant stirring (500 rpm). Then, 12 mL of aqueous ammonia solution was added dropwise to this solution under constant stirring (500 rpm) at room temperature for 5 minutes. Using a magnet, the formed

magnetite precipitate was collected and washed with deionized water until neutral pH. The washed black precipitate was mixed with 100 mL of deionized water and subjected to ultrasonic treatment (37 kHz, 110 W) under constant stirring (300 rpm) for 120 minutes. The resulting magnetite sol was afterwards cooled to room temperature. Mass concentration of the resulting magnetite sol was 2.2%.

### Preparation of healing solution

To prepare healing solution, a mixture comprising 1 mL of 20% CH solution, 2 mL of LD solution with subsequent dissolving 20 mg of CHTR and 20 mg of PRD was taken. Immediately prior to coating the wound the final solution was kept under constant stirring for 10 min and 37°C.

### Preparation of healing composite based on sol-gel magnetite

Prior to coating, 25 mL of freshly synthesized sol was mixed with 5 mL of healing solution. The produced mixture was dried in a vacuum desiccator at room temperature to a volume of 5 mL. The final composite readily produced gelled film in 5-10 min after deposition on open skin areas with an increasing viscosity from 10 mPa to 100000 mPa. The amount of drugs and matrix on the wound in this case corresponds to the values used for treating the wound with individual components.

### Wound healing tests

For wound healing test we used the method described earlier [14]. Male Wistar rats (body weight range 250–280 g) were used for the study. Animals were acclimatized under standard animal laboratory conditions for 7 days before use in the experiment. All experiments were approved by institutional animal ethical committee (Ivanovo State Medical Academy, Russia №0915) and are in agreement with the guidelines for the proper use of animals for biomedical research. Animals were divided into 4 groups, each consisting of 3 rats.

Group A: Undressed wound (Control group).

Group B: Sol-gel magnetite (Reference group).

Group C: Healing solution with drugs (Reference group)

Group D: Drugs loaded sol-gel magnetite (Test group).

Animals were anesthetized with ketamine (dose 60 mg/kg) by intraperitoneal injection, the dorsal hair was shaved and disinfected. Full thickness wounds measuring  $1 \times 1 \text{ cm}^2$  were created by excising the dorsal skin. The materials were applied on excised wounds, covered and tied with absorbent gauze to maintain the position. The wounds were treated daily with 0.5 mL of either magnetite gel or composite gel. As a reference 0.1 mL of healing solution was also used. Prior to application of medication wound area was treated with neodymium magnet to remove any unfixed magnetic residues. Wound sizes were measured daily until the healing is complete. The percentage wound reduction was calculated according to the following formula [23]:

$$C_n = [(S_0 - S_n) / S_0] \times 100 \quad (1)$$

where  $C_n$  is the percentage of wound size reduction,  $S_0$  is initial wound size,  $S_n$  is wound size on respective day.

### Characterization techniques

Specific surface areas, pore volumes and pore size distributions were determined using the nitrogen adsorption-desorption method at 77 K (Quantachrome Nova 1200 series e). Surface areas were calculated using the BET equation. Pore volumes and pore size distributions were calculated using the BJH method. Prior to analysis, the wet gels were dried at room temperature with subsequent degasation for 24 hours at room temperature. The crystal phase and crystallinity of the samples have been studied by X-ray diffraction method (Bruker D8 Advance) using Cu-K $\alpha$  irradiation ( $\lambda = 1.54 \text{ \AA}$ ), samples being scanned along  $2\theta$  in the range of  $4\text{--}75^\circ$  at a speed of 0.5 degrees per minute. Analysis of amorphous and crystalline phases was carried out with using TOPAS (Bruker) software. The samples for transmission electron microscopy (TEM) were obtained by dispersing a small probe in ethanol to form a homogeneous suspension. Then, a suspension drop was coated on a copper mesh covered with carbon for a TEM analysis (FEI TECNAI G2 F20, at an operating voltage of 200 kV). To analyze the samples using scanning electron microscopy (SEM), the obtained ground xerogel was deposited on a carbon adhesive tape and investigated without additional spraying using a Magellan 400L extra high resolution electron microscope. Zeta potential and hydrodynamic radius were measured by dynamic light scattering using a Photocor Compact-Z analyzer. XPS analysis were performed on XPS/ESCA Axis Ultra by Kratos Analytical.

### Drug release

The drug release study was carried out using HP Agilent Cary 8454 spectrophotometer. To 4 mg of dry xerogels was added 3 ml of water and light adsorption was measured in kinetic manner for 24 hours. Release of LD was detected at 218 nm, CH at 230 nm, CHRT at 220 nm and PRD at 250 nm. Calibration curve for the mixture of drugs was made by combination of calibration curves of individual components.

## Results and Discussion

From Ref. [9] we know that iron oxide nanoparticles play an important role during the wound healing process and can be observed intra- and extracellular, for instance, within the fibrin clot. At a certain time of healing process nanoparticles were cleared by macrophages and fibroblast migrating within blood flow [24]. Taking all of this into account, we have to be sure that the applied matrix is approved for parenteral injection.

Among a few dozens of crystalline phases of iron oxide, only magnetite ( $\text{Fe}_3\text{O}_4$ ) and maghemite ( $\gamma\text{-Fe}_2\text{O}_3$ ) are approved for parenteral injection [25]. According to X-ray diffraction, the main crystal phase contained in a ferric sol is magnetite, JCPDS file No. 19-0629 (Fig. 1a).

The analysis of the crystallite size carried out using the Scherrer equation indicates the presence of magnetite crystallites with an average size of  $\sim 10 \text{ nm}$  with the complete absence of amorphous phase. These results are in good agreement with XRD data for magnetite nanoparticles usually used in magnetic resonance tomography, with an average crystallite size ranging from 5 to 30 nm [26].

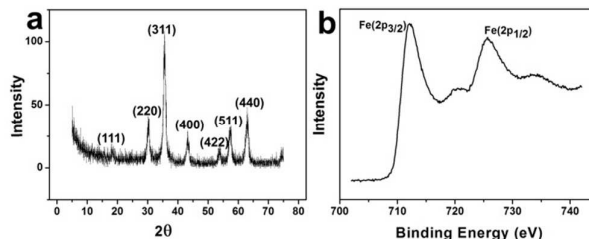


Figure 1. Confirmation of the magnetite structure: (a) XRD image of a sol-gel magnetite xerogel; (b) a high-resolution XPS spectrum of  $\text{Fe}_3\text{O}_4$ .

At the same time, the phase identification of magnetite and maghemite by the conventional X-ray diffraction method is not a simple matter because both have the same cubic structure and their lattice parameters are almost identical. For this reason, XPS measurement was conducted to identify the crystal phase of the product. Fig. 1b shows a high-resolution XPS spectrum of the pristine  $\text{Fe}_3\text{O}_4$ . The binding energy peaks at 711.5 and 725.6 eV respectively correspond to Fe 2p<sub>3/2</sub> and Fe 2p<sub>1/2</sub>, which is consistent with the oxidation state of Fe in  $\text{Fe}_3\text{O}_4$  [27].

The main advantages of nanomaterials in tissue repair are their ability to form thin films with a high specific surface area; mechanical strength and light weight, which helps prevent compression of the damaged tissue [28]. The presence of nanoparticles allows using the minimum amount of a therapeutic material to cover the maximum area of the wound, which helps protect the skin and promotes faster healing. In our case, the size of the magnetite particles is about 10 nm, which is well confirmed by electron microscopy data (Figure 2).

As shown in the HRTEM image of  $\text{Fe}_3\text{O}_4$  xerogel (Fig. 2b), the parallel lattice fringes are clearly visible (inset) for the nanoparticles, indicating the fully crystalline nanoparticles. The lattice fringe spacing (0.29 nm) displayed in the inset of Fig. 2b is in good agreement with XRD analysis (Fig.1a) of the cubic magnetite. Fig. 2c shows a SEM image with respective size distribution of the magnetite nanoparticles (Fig.2d), which are acquired from a series of SEM images. The average value of the particle size is equal to about 9.7 nm. At the same time, the hydrodynamic diameter of the magnetite nanoparticles amounted to 40 nm at a zeta potential of +32 mV.

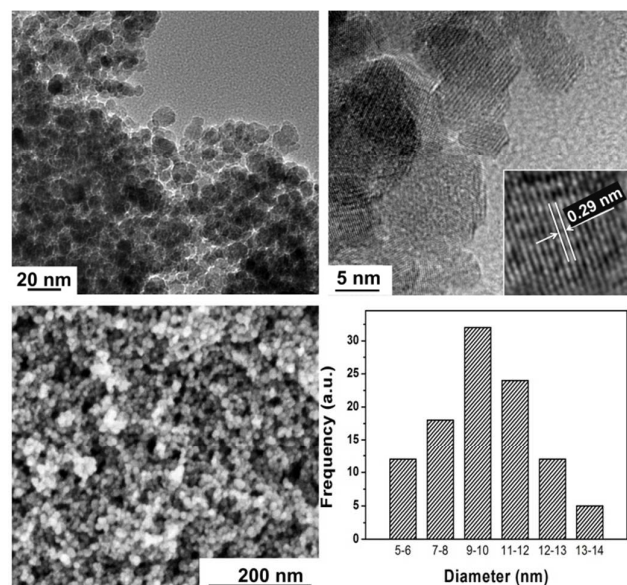


Figure 2. Demonstration of nanosize of applied magnetite particles: (a) TEM and (b) HRTEM images with lattice fringes (inset) of Fe<sub>3</sub>O<sub>4</sub> NPs; (c) SEM image with respective (d) histogram for the diameter of Fe<sub>3</sub>O<sub>4</sub> NPs.

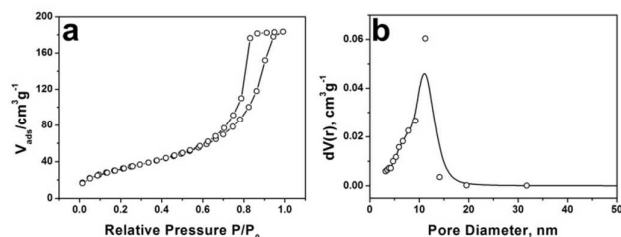


Figure 3. N<sub>2</sub> adsorption-desorption isotherm (a) and BJH mesopore size distribution (b) of magnetite biocomposite with entrapped drugs.

Given the small size of matrix nanoparticles capable of forming highly porous structures, such xerogels could be excellent drug carriers for wound-healing drugs. Drug molecules could be successfully entrapped within matrix with controlled release directly into the wound. To study the porous structure of the magnetite biocomposite with entrapped drugs, nitrogen physisorption was used.

Surface area and porosity analyses (by nitrogen adsorption, analyzed by the BET and BJH equations) were in conformity

with typical mesoporosity (Fig. 3a,b). For the magnetic composite, the values are: a surface area of 121 m<sup>2</sup>/g, a pore volume of 0.246 cm<sup>3</sup>/g and a pore size of 9.1nm. Similar numbers were obtained for pure sol-gel magnetite: a surface area of 119 m<sup>2</sup>/g, a pore volume of 0.261 cm<sup>3</sup>/g and a pore size of 8.9 nm. The pores of this size will allow for a rapid release of small drugs and provide a prolonged release of macromolecules, such as proteins and peptides. To confirm this, we have studied release of drugs from a porous composite at a pH of 7.4 (Fig. 4a). The release rate was measured for 24 hours due to everyday repeated treatment of wounds.

In general it can be noted that the release rate also correlates well with the molecular weight of released substance. The highest rate of release is provided by LD and CH. Despite the similar molecular weight, PRD is released slowly because of its poor solubility and hydrophobicity. The lowest release rate is demonstrated by CHRT.

Wound-healing composition was selected in such a way as to provide the most effective healing conditions. In proposed composite release profile of drugs was carried out in conformity with the wound healing process. After formation of gel film on the wound surface about 50% of painkiller (LD) and antibacterial agent (CH) releases during the first 20 min, thus providing immediate removal of pain and preventing the formation of bacteria colonies both directly at the wound and at the dressing material. The remaining amount of LD and CH released at a much slower rate providing a long-term effect. Prednisolone and chymotrypsin released more uniformly. 30% of prednisolone release during the first 5 hours, thereby preventing the development of unwanted immediate and long-term inflammatory reactions, which might lead to the development of scar tissue and an increase in its size. Release of the necrolytic drug (CHTR) proceeded at the final stage following the formation of a scab and tissue necrosis.

Taking into account paper [29] on cytotoxicity of magnetite NPs we can conclude that the method for producing magnetite hydrosol developed in this paper could provide high cells viability by some reasons: we didn't use peptizers to stabilize NPs thus pH of our magnetite sol is neutral, we also didn't use stabilizers which can cause specific cell adsorption to the

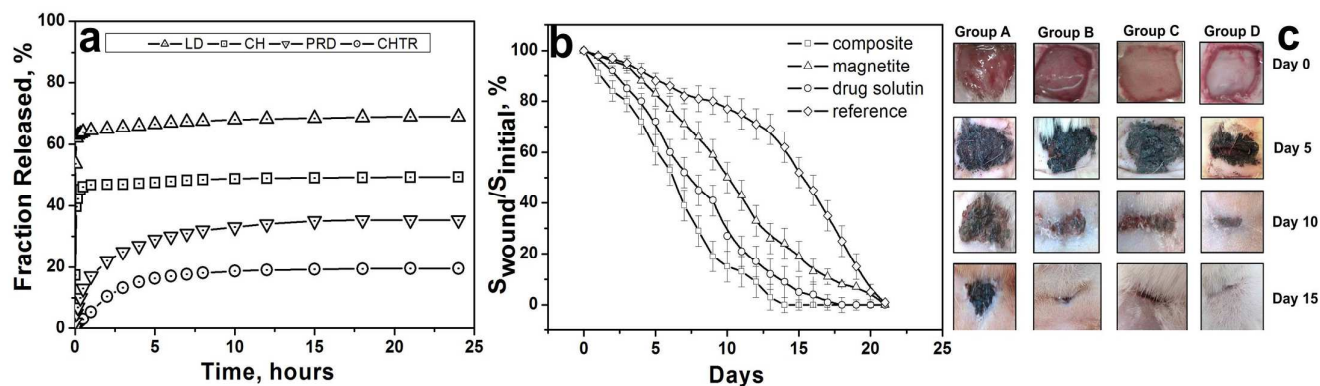


Figure 4. Release kinetics of respective drug molecules from sol-gel magnetite (a) at pH = 7.4. Kinetic curves of variations in area of experimental full thickness wounds under treatment with respective group (b). Illustration of the temporal development of the tissue repair process according to respective group.

surface of nanoparticles and our magnetite is quite stable in high ionic media and no release of toxic Fe ions was observed. According to atomic absorption spectroscopy, the presence of the Fe<sup>3+</sup> and Fe<sup>2+</sup> ions in Ringer's solution after 30 days of exposure of magnetite NPs was not detected.

Further experiments dealt with *in vivo* tests. Four groups of rats were used as indicated in *Materials and Methods* Section. Fig. 4b shows the kinetic curves for the change in the wound areas during healing. One can see that experimental full-thickness wounds treated with the composite are completely healed in 14 days. Wound healing for the control group occurs only after 21 days. Treating with healing solution promotes a decrease in complete wound healing time by 4 days (17 days of healing). Magnetite coating as wound healer makes healing process more uniform, but finally stays at the same period as the control group thus magnetite NPs are practically fully inert and have low healing ability. Nevertheless, uniformity of healing process provided by magnetite NPs is related with mechanical features of formed xerogel film. Because of capillary effect arising due to drying of magnetite film, contraction of the wound area occurred, resulting more uniform healing and smaller scar size.

Considering the classic mechanisms of wound healing [30], we can assume the reasons for accelerating the wound healing process in the magnetite biocomposite. Immediately after the injury the stage of hydration occurs, or self-cleaning. Excess moisture is absorbed by the magnetite hydrophilic matrix. As a result, a rapid release of anesthetic (LD) and antimicrobial (CH) agents begins. Hydration takes place against the background of inflammatory reaction and is characterized by complex morphological, biochemical, chemical and physical changes occurring in response to the injury. At the same time, magnetite due to its high biocompatibility acts as a granulation tissue, filling the entire wound cavity.

Magnetite coating is a mechanical and physiological barrier preventing the spread of germs from the wound into the surrounding tissue and absorbing toxic products of tissue decay, bacteria and toxins. Subsequently, granulation magnetite tissue turns into scar connective tissue, which is covered by epithelium on the outside. In order to neutralize the inflammatory processes, thereby reducing the size of scar tissue, prednisolone gradually releases. Prednisolone suppresses functionality of tissue macrophages, restricts the migration of leukocytes to the inflammation area, and contributes to the stabilization of lysosomal membranes, thereby reducing the concentration of proteolytic enzymes in the inflammation area. All of these processes take place against the background of inflammation, and are accompanied by suppuration arising from infection of the wound. Following this, degenerative and necrotic processes develop in damaged tissues, which are accompanied by the formation of purulent exudate, i.e., the wound is gradually cleared from the degeneration and necrosis products. At the same time, CHRT (necrolytic agent), whose release is slowest, takes its action. Release of CHRT in the wound compensates the lack of proteolytic enzymes, whose formation was blocked by PRD. Already on the first days the cellular elements (fibroblasts,

capillary endothelium) and wound hormones (necrotin, metabolin) begin to grow and reproduce, thus stimulating the regenerative processes. Thus, it becomes clear that the use of the individual components (magnetite matrix, drug healing solution) can solve problems only partially. The maximum rate of wound healing in the magnetite biocomposite is achieved due to its complex effect on the whole process of wound healing, participating in each of the stage.

Following optimal healing process, the scar decrease has been also observed. On the 40<sup>th</sup> day of the healing the size of scars among all of the groups was measured. According obtained results, the scar in the group with composite was almost 2.1 times smaller than control group (1.3 and 1.6 for group B and C respectively). We believe that scar size decrease is accompanied with described mechanism of wound healing and associated with the minimal inflammatory response when the composite is used.

In addition to the fact that magnetite itself is capable to participate efficiently enough in the wound healing process, another unique feature, which would be of use in cleaning wounds, is its magnetosensitivity. We assume that the same materials can be used not only as efficient dressing wound-healing materials, but also as pre-cleaners and hemostatics, since after application they might be separated with a magnet, having absorbed poisons, toxins and other contaminating substances. We plan to continue these studies and present the results in our future publications.

## Conclusions

In this study we report having developed efficient wound-healing materials based on drug entrapped magnetite xerogels. Compared to the control group, there is a 1.5-fold increase in wound healing rate (21 and 14 days for complete healing, respectively) as well as strong size scar decrease (2.1 times smaller). This result was achieved through the optimal release of entrapped healing drugs (LD, CH, PRD, CHRT). For these materials we release of medicines was carried out in strict conformity with the wound healing process. Large portions of painkiller and antibacterial agent released during the first minutes provide immediate removal of pain and prevent the formation of bacteria colonies both directly at the wound and at the dressing material. Prednisolone uniformly released during the first 5 hours, thereby preventing the development of inflammatory reactions. Release of the necrolytic drug proceeded at the final stage following the formation of a scab and tissue necrosis. Since magnetite nanoparticles are completely biocompatible and biodegradable, we believe that these materials can also be efficient in the treatment of infectious and chronic wounds.

## Acknowledgements

This work was supported by the Russian Government, Ministry of Education. (Research was made possible due to financing provided to the Customer from the federal budget aimed at

maximizing Customer's competitive advantage among world's leading educational centers).

The authors are grateful to the Center for Nanoscience and Nanotechnology in Hebrew University for assistance in performing TEM, SEM and XPS experiments.

## References

- Chandan K. Sen, Gayle M. Gordillo, Sashwati Roy, Robert Kirsner, Lynn Lambert, Thomas K. Hunt, Finn Gottrup, Geoffrey C. Gurtner and Michael T.. *Wound Repair and Regeneration*, 2009, **17**, 763–771.
- S. Petrulyte, *Dan. Med. Bull.*, 2008, **55**, 72–77.
- I. Firkowska, S. Giannona, J. A. Rojas-Chapana, K. Leucke, O. Brustle, M. Giersig, *Nanomaterials for Application in Medicine and Biology*, 2008, 1–15.
- A. V. Singh, W. N. Gade, T. Vats, C. Lenardi, P. Milani, A. S. Aditi, *Cur. Nanosci.*, 2010, **6**, 577–586
- R. Bhattacharya, P. Mukherjee, *Adv. Drug Delivery Rev.*, 2008, **8**, 1289–1306.
- G. Mohammad, V. K. Mishra, H. P. Pandey, *Dig. J. Nanomater. Biost.*, 2008, **3**, 159–162.
- K. K. Y. Wong, X. Liu, *MedChemCommun.*, 2010, **1**, 125–131.
- A. A. Rakhmetova, T. P. Alekseeva, O. A. Bogoslovskaya, I. O. Leipunskii, I. P. Ol'khovskaya, A. N. Zhigach, N. N. Glushchenko, *Nanotechnol. Russ.*, 2010, **5**, 271–276.
- O. Ziv-Polat, M. Topaz, T. Brosh, S. Margel *Biomaterials*, 2010, **31**, 741–747.
- C. J. Ingham, J. Maat, W. M. Vos, *Biotechnol. Adv.*, 2012, **30**, 1089–1099.
- C. Sun, J.S.H. Lee, M. Zhang, *Adv. Drug Delivery Rev.* 2008, **60**, 1252–1265.
- L. Gu, R. H. Fang M. J. Sailor, J. H. Park, *ACS Nano.*, 2012, **6**, 4947–4954.
- R. J. Mitkus, D. B. King, M. A. Hess, R. A. Forshee, M. O. Walderhaug, *Vaccine*, 2011, **29**, 9538–9543.
- K. V. Volodina, N. L. Solov'eva, Vasilii V. Vinogradov, V. E. Sobolev, A. V. Vinogradov, Vladimir V. Vinogradov. *RSC Advances*, 2014, **4**, 60445–60450.
- A. Moore, E. Marecos, A. Bogdanov Jr., R. Weissleder, *Radiology*, 2000, **214**, 568–574.
- R. A. Petros, J. M. Desimone, *Nat. Rev. Drug Discovery*, 2010, **9**, 615–627.
- J.S. Boateng, K.H. Matthews, H.N.E. Stevens, G.M. Eccleston, *J. Pharm. Sci.*, 2008, **97**, 2892–2923
- K. Shimizu, A. Ito, H. Honda *J. Biomed. Mater. Res., Part B*, 2006, **77B**, 265–272,
- E. Eroglu, F. Eroglu, F. Agalar, I. Altuntas, R. Sutcu, D. Ozbasar, *European Journal of Emergency Medicine*, 2001, **8**, 199–201.
- J. Ramundo, G. Mikel, *J. of WOCN*, 2008, **35**, 273–280.
- A. Kumar, A. S. G. Curtis, *J. Mater. Sci.: Mater. Med.*, 2004, **15**, 493–496.
- B. M. Holzapfel, J. C. Reichert, J. T. Schantz, U. Gbureck, L. Rackwitz, U. Nöth, F. Jakob, M. Rudert, J. Groll, D. W. Hutmacher, *Adv. Drug Delivery Rev.*, 2013, **65**, 581–603.
- S.N. Park, H.J. Lee, K.H. Lee, H. Suh, *Biomaterials*, 2003, **24**, 1631–1641.
- B. S. Zolnik, A. G. Fernandez, N. Sadrieh, M. A. Dobrovolskaia, *Endocrinology*, 2010, **151**, 458–465.
- S. Fütterer, I. Andrusenko, U. Kolb, W. Hofmeister, P. Langguth, *J. Pharm. Biomed. Anal.*, 2013, **86**, 151–160.
- Y. W. Jun, Y. M. Huh, J. S. Choi, J. H. Lee, H. T. Song, S. Kim, S. Yoon, K. S. Kim, J. S. Shin, J. S. Suh, J. Cheon. *J. Am. Chem. Soc.*, 2005, **127**, 5732–5733.
- X. W. Teng, D. Black, N. J. Watkins, Y. L. Gao, H. Yang, *Nano Lett.*, 2003, **3**, 261.
- Z. Fan, B. Liu, J. Wang, S. Zhang, Q. Lin, P. Gong, L. Ma, S. Yang, *Adv. Funct. Mater.*, 2014, **24**, 3933–3943.
- M. Mahmoudi, A. Simchi, M. Imani, M.A. Shokrgozar, A.S. Milani, U.O. Häfeli, & P. Stroeve, *Colloids and Surfaces B: Biointerfaces*, 2010, **75**, 300–309.
- A. J. Singer, R. A. F. Clark, *N. Engl. J. Med.*, 1999, **341**, 738–746